Contrasting H-etching to OH-etching in plasma-assisted nucleation of carbon nanotubes

Contrasting H-etching to OH-etching in plasma-assisted nucleation of carbon nanotubes

Phaedra Van de Sompel[1], Umedjon Khalilov[1,2] and Erik C. Neyts[1,*]

[1]PLASMANT research group, NANOLab Center of Excellence, University of Antwerp, Universiteitsplein 1, 2610 Antwerp, BELGIUM

[2]Institute of Ion-Plasma and Laser Technologies, Academy of Sciences of the Republic of Uzbekistan, 33 Durmon Yuli Street, Tashkent 100125, UZBEKISTAN

* Corresponding author. Tel. +32 3 820 23 88. E-mail: erik.neyts@uantwerpen.be (Erik C. Neyts)

Abstract

In order to gain full control over the growth of carbon nanotubes (CNTs) using plasma enhanced chemical vapour deposition (PECVD), a thorough understanding of the underlying plasma-catalyst mechanisms is required. Oxygen containing species are often used as or added to the growth precursor gas, but these species also yield various radicals and ions which may simultaneously etch the CNT during the growth. At present, the effect of these reactive species on the growth onset has not yet been thoroughly investigated. We here report on the etching mechanism of incipient CNT structures from OH and O radicals as derived from combined (reactive) molecular dynamics (MD) and force bias Monte Carlo (tfMC) simulations. Our results indicate that the oxygen containing radicals initiate a dissociation process. In particular, we show how the oxygen species weaken the interaction between the CNT and the nanocluster. As a result of this weakened interaction, the CNT closes off and dissociates from the cluster in the form of a fullerene. Beyond the specific systems studied in this work, these results are generically important in the context of PECVD-based growth of CNTs using oxygen-containing precursors.

1. Introduction

Following the discovery of carbon nanotubes (CNT)[1, 2], their extraordinary properties[3-6] have been the subject of many research projects. In particular, control over their chiral-dependent properties, such as the electronic and thermal conductivities,[6-8] is of a great interest. These properties are a direct result of the growth mechanism, which is determined by the synthesis technique. Among various CNT synthesis techniques, arc-discharge [7, 9], laser ablation [10, 11] and chemical vapour deposition methods [12, 13] are the most widely used. Both thermal chemical vapour deposition (CVD) and plasma-enhanced CVD (PECVD) techniques still hold great promise for reaching this goal.[12, 14, 15] In particular, PECVD offers potential for growth control, since it offers some advantages over thermal CVD such as its use of lower temperatures and ability to grow vertical aligned CNTs.[13] However, PECVD also shows several disadvantages in comparison to thermal techniques. In particular, under plasma conditions, the carbon structures are exposed to high fluxes of highly reactive radicals and ions, which may etch and sputter the growing strutures.[16] As a result, the net growth kinetics of the CNTs can be understood as a balance between growth and removal processes.[14-17]

The dual role of hydrogen has already been explored in several previous studies, both experimental[18-20] and computational [17, 21] and is reasonably well-understood. Hydrogen can enhance or prevent the CNT growth regarding its concentration in the system.[22] A study by Zhang et al. compared different growth conditions of the vertically aligned SWCNTs.[20] They report that the reactive hydrogen species generally have a negative effect on the formation of SWCNTs and repeat again that they also etch the fully realised SWCNT. Namely, H-atoms contribute to the etching process of CNTs by causing their sp^2 C-C bonds to break. Behr et al. reported that hydrogen atoms preferably amorphize and subsequently etch graphite and CNTs.[18] This selective etching can be utilized as a way to eliminate unwanted carbon structures or to separate the different types of conducting nanotubes as shown by Zhang et al. and Hou et al.[19, 23]

A plasma environment also often contains oxygen atoms and other oxygen-containing species, as they are added in the form of alcohols or water in thermal CVD to obtain a higher CNT yield. In the same study Zhang et al. also state the role of oxygen as a hydrogen scavenger.[20] They observed a positive effect on the growth because it can counter the high concentration of reactive hydrogen present in PECVD. Zhang and co-workers conducted several PECVD growth experiments in

which they found that without O_2 in the feedstock there was a significant decrease in high-yield nanotube formation. This would confirm that oxygen is removing the hydrogen atoms from the CNT surface and in turn shifting the C/H·balance to favour the growth.

In the same vain as with the H_2 species, a number of studies have shown the usage OH or O species as a way to selectively grow semiconducting CNTs.[21, 24-27] Most often it is added water vapour in a CVD setup that decomposes to form OH radicals. But also species such as isopropyl alcohol and carbon monoxide have proven to give similar results.[26, 27] These oxygen containing species are shown to mostly etch semiconducting nanotubes during the growth stage. The explanation for this selectivity is that the chirality of the CNT is related to the chemical stability and more importantly to the interfacial formation energy between the catalyst and the carbon structure.[28, 29] The catalyst is thus an important factor in the etching process of OH species. Yang et al. specifically employed this aspect to form their desired catalysts.[30] In addition, Zhou et al. have also shown that the etching effect only occurred in the catalyst area. Moreover, they proposed that there are certain rules that need to be followed to get an efficient selection of nanotubes.[25] When the water concentration during the growing process is too high, only a very limited amount of CNTs are formed.[26] The reactive species most likely etch the growing network before it can assemble a stable structure. The same Goldilocks principle was observed with O_2 when working with a floating catalyst.[28]

Important to note is that in all these experimental studies, the effect of the OH species was not singled out, but involve many different parameters such as the carbon feed rate, contributing to the overall result. Still, detailed knowledge on the molecular level of the influence of oxygen species on the CNT growth process is much scarcer than for hydrogen.

While the macroscopic mechanisms of thermal CNT nucleation from oxygen-containing hydrocarbon feedstocks has been recently elucidated,[22] at present, however, more detailed atomistic studies aimed at a more precise understanding of the role of oxygen species in the plasma CNT growth process have not yet been reported. [20, 31, 32] Also the effect of oxygen species on the nucleation of carbon nanostructures in PECVD has not yet been thoroughly studied.

In this work, we aim to partially close this knowledge gap. In particular, we study the etching mechanisms of different caps and incipient nanotubes from oxygen species, such as O and OH in a comparison with H atoms, using a hybrid Molecular Dynamics and Monte Carlo (MD/tfMC)

technique, in order to better understand the mechanisms underpinning the nucleation and growth of CNTs in a plasma environment.

2. Computational details

All simulations in this work are performed using a combined (reactive) Molecular Dynamics (MD) and time-stamped force-bias Monte Carlo (tfMC) technique.[33, 34] The interactions between the atoms are described by the ReaxFF force field, using parameters by Zou et al.[35] developed for a Ni/C/H/O system. All initial carbon nanostructures, i.e., (5,5) and (10,0) carbon cap and tube, are attached on a $Ni_{55}C_x$ nanocluster (according to VLS mechanism [36]). The structures are subsequently thermalized prior to oxidation. During the thermalization, the temperature is kept constant by the canonical Bussi thermostat[37] at either 800 K or 1600 K. The $Ni_{55}C_x$ nanocatalyst is physisorbed on a virtual substrate employing a z-integrated Lennard-Jones potential.[38] While both nanotubes initially mismatch with a icosahedron Ni particle[39], the particle becomes amorphous due to the Gibbs-Tomson effect (i.e., depression of a melting temperature) as well as the substrate-catalyst interaction [40, 41].

During the simulations, reactive oxygen species (O or OH) are inserted in the simulation box one by one and their total density in the gas-phase (10 atoms/(40×40×40) Å) is kept constant. When an oxygen species attaches to the carbon nanostructure or the nanocluster, the tfMC simulation takes over to relax the resulting structure. During the relaxation, no new atoms or molecules are allowed to enter the simulation box. During the simulation, the etching products are removed every 10^6 MD steps to prevent pyrolysis reactions in the gas-phase.

3. Results and discussion

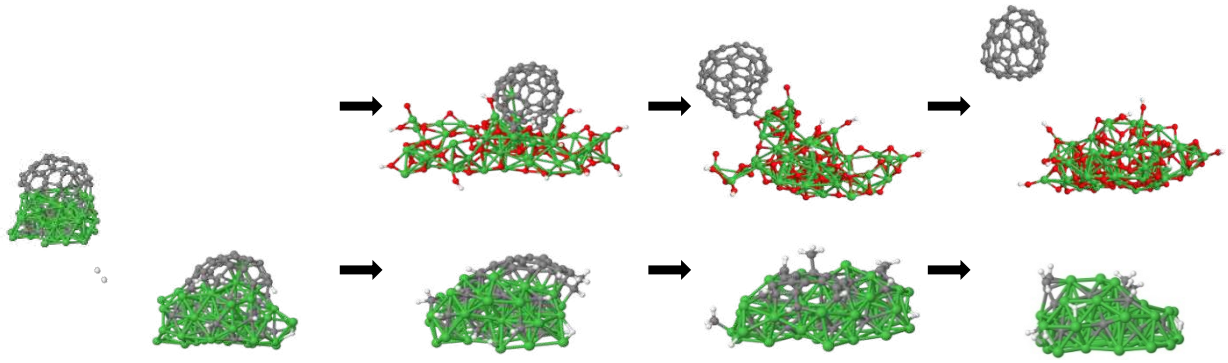

Figure 1. The detaching/etching stages of carbon cap in the case of OH (above) or H radicals (below).

Structure removal. Figure 1 demonstrates the detaching/etching process of a carbon cap of a (5,5) CNT due to OH and H radicals. In our previous studies, we mechanistically studied H-based etching of a carbon cap.[14, 15, 17] In this case, the cap converts to a carbon sheet during the hydrogenation. After the complete etching of the structure (such as a carbon sheet and chains) as a C_xH_y molecules/radicals, the Ni nanoparticle with dissolved C atoms remains attached to the substrate.

However, as shown in Figure 1, the simulations demonstrate that the nature of the removal process of the cap using oxygen (O or OH) species is different than in the case of hydrogen species. In this case, the carbon structure eventually detaches as a fullerene from the substrate-bounded pure Ni nanocluster. To understand these different etching mechanisms, we analyse the following key phenomena during the oxidation/hydroxylation in comparison with hydrogenation.

Initial reactions. We observe that both OH and H radicals preferentially attach to the nickel nanocatalyst, rather than to the carbon cap. While the hydrogen atom then either diffuses towards the cap-catalyst interface or finds another adsorbed H atom and desorbs as H_2 molecule (i.e., Langmuir-Hinshelwood mechanism [42]), the oxygen atoms prefer to remain dissolved in the nickel cluster after recombination of two adsorbed OH radicals. In particular, the Ni catalyst facilitates the recombination reaction, i.e., $OH+OH \rightarrow H_2O\uparrow+O$, which mainly results in desorption of H_2O molecules. The results show that H_2O molecules comprise on average about 90% of all desorbing gas-phase species in the case of OH, while in the H case practically 100% of the desorption products is H_2 (see Table 1). Although the fractions of other desorbed H_xO_y and etched C_xH_y or $C_xH_yO_z$ species are non-zero, H_2O in the OH case and H_2 in the H case are main species in the gas-

phase.

Table 1. The number of desorbed or etched species found in the gas-phase during the OH cases (left) and the H cases (right).

H_2O	414	86.61	H_2	1781	97.32
O_2	27	5.65	CH_4	42	2.30
CO	20	4.18	CH_3	6	0.33
O	7	1.46	CH	1	0.05
CO_3	4	0.84			
HO_2	3	0.63			
CO_2	2	0.42			

Because of their high density in the OH case, the water molecules frequently re-adsorb, much like the recombination of H-atoms and (re-)desorption of H_2 molecules in the H case. However, due to the high dissociation barrier of a water molecule on a Ni cluster (~1.25 eV),[22] O atoms rarely re-dissolve into the nanocluster after H_2O re-adsorption without an energetic barrier. In contrast, re-adsorbed H_2 molecules dissociate relatively easily. Indeed, the dissociation barrier of H_2 on a Ni cluster is only approximately 0.56 eV.[22]

Consequently, the amount of re-adsorbed H atoms can increase relatively easily, which leads to enhancing the H-etching process. Opposite to this are the non-dissociated oxygen species like H_2O, which rather cause a delay in the oxygen-based etching process, neither adding nor removing atoms from the cluster or from the CNT cap structure. This corresponds with previous studies in which water molecules are added as a growth enhancer.[43, 44]

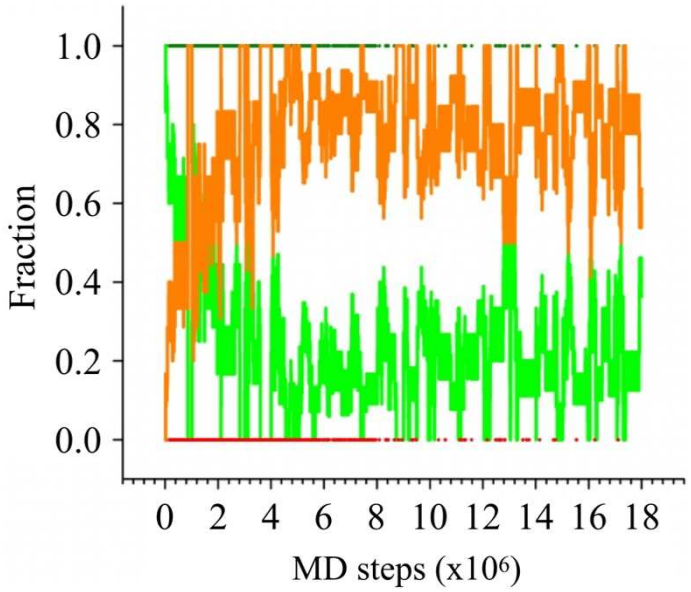

Figure 2. The fraction of C-H (orange for H case and red for OH case) and Ni-H (light green for H case and dark green for OH case) bonds as a function of the number of MD steps.

Adsorbed H atoms. We find H atoms as the only adsorbed species in the H case. We find that after a catalytic dissociation of adsorbed H_2 on the Ni cluster, the H adatoms diffuse towards the CNT rim and form H-C bonds at the tube-cluster interface. In particular, Figure 2 shows that the fraction of H adatoms connected to the cap (i.e., H-C bonds) rises while their fraction on the catalyst surface (i.e., H-Ni bonds) decreases as a function of time. Consequently, such H connections to interface C atoms weaken the neighbouring C-C bonds. In particular, H-C bonds results in more stress on

the ortho C-C bonds in the cap structure and consequently cause the C-C bond to break, which is considered as the etching onset. [17] As a result carbon atoms are one by one removed from the CNT structure, and the etched species are found in the gas-phase.[15]

On the other hand, in the OH case, O species are mostly found as water, as mentioned previously. In this case, most H atoms are removed due to the H_2O desorption. Nonetheless, some H atoms can remain on the catalyst surface due to the $OH+OH \rightarrow HO_2\uparrow+H$ reactions, although its frequency of occurrence is low (0.72% over all events). The remaining hydrogen atoms are thus only very rarely found on the nickel particles before they desorb as either H_2 or H_2O. Consequently, such desorption brings their concentration at the tube-catalyst interface and on the cap structure to practically zero. Therefore, the H adatoms in Figure 2 are only observed on the Ni particle. Due to this behaviour, the etching rate of carbon structures by H atoms is negligible in the OH case.

Ni oxide nanoclusters. In the OH case, active water formation leads to a large fraction of dissolved oxygen atoms, which oxidize and structurally modify the Ni_{55} nanocluster. This phenomenon can be connected to the experimental finding[45] that Ni nanoparticles smaller than 5.5 nm burn up completely during the oxygen treatment, even at low temperature (<600 K). The number of dissolved O atoms keeps rising until saturation. As a consequence, their interactions with nickel atoms lead to swelling of the nanocluster. [46] In particular, the Ni-Ni distance in the origin cluster (with a radius of 5 Å) increases in the NiO cluster (with a radius of 6.58 Å) about 1.3 times. The shape of the 1 nm-diameter nanoparticle is already stressed due to the Gibbs-Tomson effect[40, 41] but changes completely during the oxidation. We mostly find either NiO or Ni_2O_3 clusters amongst other minor oxides (see Supplementary Figure 2). In the Ni_xO_y cluster, the formation of Ni-O bonds, which are stronger than Ni-C bonds, [47, 48] significantly weakens the interaction between the oxidized nickel cluster and a carbon cap or tube. In particular, the interaction energies for Ni-CNT(5,5) and NiO-CNT(5,5) are -3.69 eV and 8.26 eV, respectively. Also, the adsorption energy difference for the (10,0) tube on the pristine Ni-cluster and the NiO-cluster is 14.29 eV (see Supplementary Table 1). The results indicate that while the interaction energy between the nanotube rim and the pure Ni nanoparticle (for (5,5)@Ni_{55} and (10,0)@Ni_{55} equal -3.69 eV and -5.73 eV, respectively) depends on the tube chirality, which is in qualitative agreement with quantum-mechanical calculation results[29], while the interaction energy does not strongly depend on the chirality when the tube connects to the oxidized Ni nanoparticle (with energy differences

of ~0.3 eV). Consequently, this phenomenon leads to the (oxide) catalyst inactivity in SWNT growth selectivity[49] which is in agreement with experimental observations[50].

Dissolved-to-ring carbon. During the oxidation of the Ni cluster, dissolved C atoms diffuse toward the cap rim due to weakening of the Ni-C bonds. Figure 3a shows the decrease in the number of dissolved carbon atoms (dissolved C) while the number of C atoms in the carbon cap (ring C) increases.

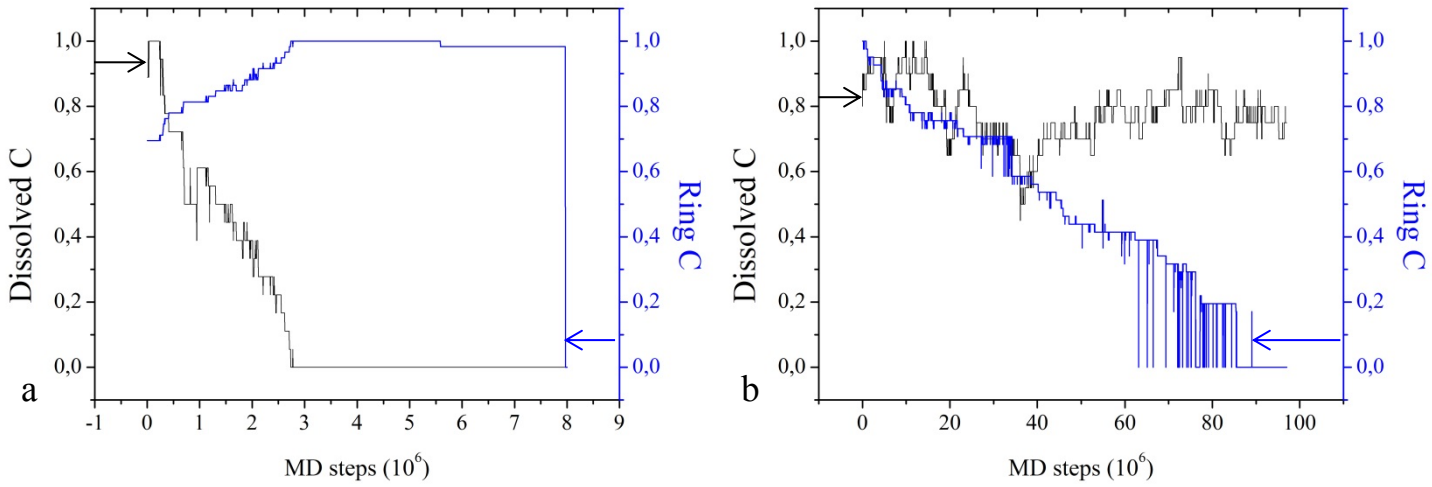

Figure 3. The relative number of different types of carbon atoms as a function of MD steps for the OH case (3a) and H case (3b). The initial amount of C atoms is 59 for both cases.

On the other hand, in the H case (Figure 3b), we can only see a decreasing trend for the ring C atoms, i.e., the dissolved C atoms do not transform into ring C atoms. Furthermore, the number of dissolved C remains constant. This indicates that the carbon structure (ring C) gradually loses its C atoms, i.e., the structure is gradually etched. In contrast, in the OH case, the carbon cap on the NiO-nanocluster detaches. This can be explained by the active transformation of dissolved C atoms into ring C atoms, leading to blocking off the cap rim by a carbon network, thus necking the carbon cap.[22] Eventually, the cap converts to a fullerene molecule.

As mentioned above, the interaction energy of the carbon structure with the NiO cluster is lower than the interaction with the Ni nanocluster. Therefore, the formed fullerene eventually detaches from the NiO surface. Zhang et al. observed the termination and detachment of SWCNTs on a Co/MgO catalyst. [51] They propose that the necking is due to a broken carbon cycle where the incorporation rate of carbon atoms (C_{inc}) is faster than the limited supply of active carbon species

(C_{sup}). Accordingly, the incorporation rate of the dissolved C atoms into the cap (tube) structure is considerably higher in our case due to extensive formation of Ni-O links. Such imbalance results in the weakened tube-catalyst interface causing the detachment of the CNT cap. In some cases, the incorporation rate of O into the cap (tube) rim is higher than the incorporation rate of dissolved C atoms. Consequently, C atoms in the cap (tube) rim bind to O atoms instead of to dissolved C atoms. When numerous O atoms can bind to the base of the cap (tube), the carbon structure cannot close off to form a closed or opened fullerene-like structures. When this O-terminated carbon cap (tube) detaches from the cluster surface, the cap (tube) is subsequently damaged and/or destructed (see Supplementary figure 1).

OH vs O. In the case of OH impact, the main remaining species on and in the nanocatalyst is the O atom, as discussed before. When we compared the effects of OH and O radicals, we found that the O radicals initiate the O dissolution faster than the OH radicals. The delay in the OH case is explained by the OH+OH recombination time before they desorb as a H_2O molecule. In case of the O radical, the O atom dissolves into the cluster rather than diffusing on the surface and recombining with another adsorbed O atom. Therefore, O_2 molecules are not the dominating desorbing gas-phase species in the O case like desorbing H_2O is in the OH case or desorbing H_2 is in the H case. As a result, the nickel nanocluster reaches its saturation point faster in the O case. After saturation, O atoms cannot dissolve further inside the cluster and will thus recombine with other O adatoms before leaving the surface as O_2 molecules.

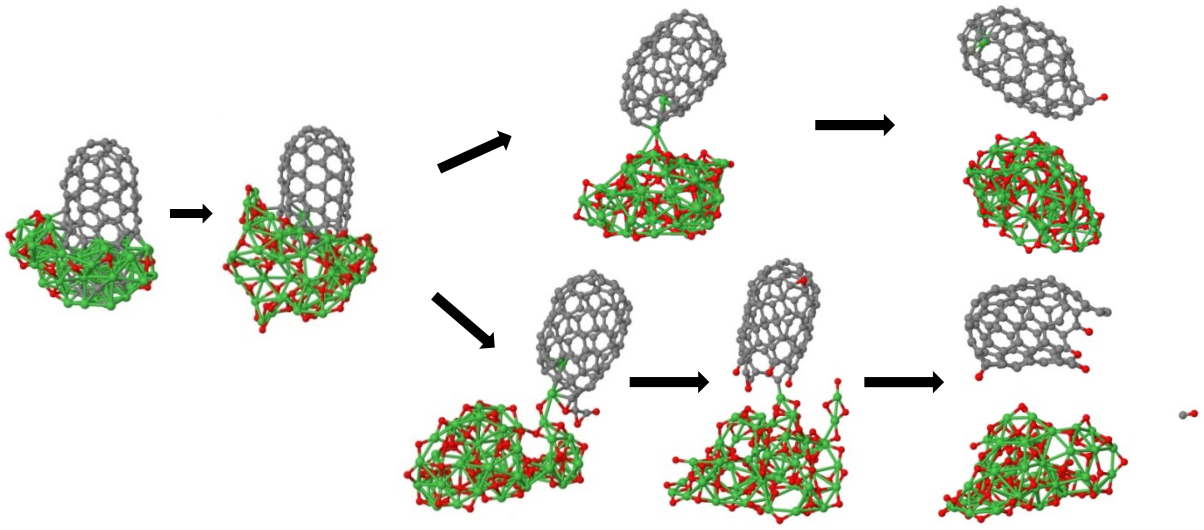

Figure 4. Two scenarios of the detachment of small CNTs.

Overall, we find two possible scenarios for CNT detachment, as depicted in Figure 4, viz. (1) CNT detachment as a fullerene in the both OH and O cases and (2) detachment of an O-terminated CNT in the O case. In the first scenario, the O dissolution rate is lower than the incorporation rate of dissolved C atoms into the CNT rim due to OH+OH or O+O recombination, while it can be faster in the second scenario due to fast O dissolution. Consequently, O-atoms forming bonds to ring-C atoms can occur in the second case. This phenomenon can be connected to the experimental evidence that the residual oxygen in the catalyst suppresses tube growth[50]. After saturation, O adatoms can also attack the CNT rim which is not entirely closed off by a carbon cage. Based on these two scenarios, either the dissociation takes place quickly or the oxygen atoms can bind to the carbon structure and cause etching pits and/or etch the bottom of the fullerene molecule before dissociating. After the oxidation (in both OH and O cases), the interaction between the nanocatalyst and the O-terminated CNT or the fullerene becomes weak and unstable (see Supplementary Table 1). The tube detachment or spontaneous cap formation due to a weak nanocatalyst - SWNT binding strength was elucidated by Ding and colleagues as well[52]. Namely, the reactivity of the nickel nanocluster is reduced and it eventually entirely transforms to a nickel oxide ($Ni_{55}O_x$) nanocluster. Consequently, the oxidation leads to detachment of the carbon structure from the poisoned nanocatalyst, as discussed above.

4. Conclusions

Using combined MD/MC simulations, we study the oxidation and subsequent dissociation of carbon nanotube caps and small carbon nanotubes. The initial hypothesis that the effect of oxidation is similar to the hydrogenation etching effect, was proven incorrect. While the H atoms prefer to bind to the carbon atoms and etch away the structure, O atoms mainly stay in the nickel catalyst and oxidize the cluster. As a result, the H radicals destroy the carbon structure while leaving only the nanocluster intact, while – in contrast – the O radicals saturate the nanocluster and the carbon structure dissociates from the cluster, remaining largely intact.

We also calculated the interaction-energy between the CNT and the cluster before and after the oxidation of the nanocluster. These results also indicate that the lowered interaction causes the dissociation of the carbon structure. Overall, the H radicals etch away the carbon structure and do not influence the interaction between catalyst and CNT. In contrast, the addition of OH radicals causes the CNT to be removed from the nanocluster while keeping the structure largely intact. In general, this study leads to a better understanding of the effect of oxygen radicals on the CNT growth in a plasma environment.

5. Acknowledgments

The authors gratefully acknowledge the financial support from the Fund of Scientific Research Flanders (FWO), Belgium, Grant number 12M1318N. The work was carried out in part using the Turing HPC infrastructure of the CalcUA core facility of the Universiteit Antwerpen, a division of the Flemish Supercomputer Centre VSC, funded by the Hercules Foundation, the Flemish Government (department EWI) and the Universiteit Antwerpen. The authors also thank Prof. A. C.T. van Duin for sharing the ReaxFF code.

References

1. Iijima, S., Helical microtubules of graphitic carbon. *Nature* **1991,** *354* (6348), 56-58.
2. Iijima, S.; Ichihashi, T., Single-shell carbon nanotubes of 1-nm diameter. *Nature* **1993,** *363* (6430), 603-605.
3. Iizumi, Y.; Yudasaka, M.; Kim, J.; Sakakita, H.; Takeuchi, T.; Okazaki, T., Oxygen-doped carbon nanotubes for near-infrared fluorescent labels and imaging probes. *Sci Rep* **2018,** *8* (1), 6272.

4. Loos, M. R.; Nahorny, J.; Fontana, L. C., Plasma Modification of Carbon Nanotubes. *Curr. Org. Chem.* **2013,** *17*, 1880-1893.
5. Khan, W.; Sharma, R.; Saini, P., Carbon Nanotubes - Current Progress of their Polymer Composites. In *Carbon Nanotube-Based Polymer Composites: Synthesis, Properties and Applications*, Berber, M. R.; Hafez, I. H., Eds. IntechOpen, 2016.
6. Ibrahim, K. S., Carbon nanotubes-properties and applications: a review. *Carbon Lett.* **2013,** *14* (3), 131-144.
7. Monthioux, M.; Serp, P.; Flahaut, E.; Razafinimanana, M.; Laurent, C.; Peigney, A.; Bacsa, W.; Broto, J.-M., Introduction to carbon nanotubes. In *Springer Handbook of Nanotechnology*, Bhushan, B., Ed. Springer Handbooks: 2010; pp 47-118.
8. Saito, R.; Fujita, M.; Dresselhaus, G.; Dresselhaus, M. S., Electronic structure of chiral graphene tubules *Appl. Phys. Lett.* **1992,** *60* (18), 2204 - 2206.
9. Prasek, J.; Drbohlavova, J.; Chomoucka, J.; Hubalek, J.; Jasek, O.; Adam, V.; Kizek, R., Methods for carbon nanotubes synthesis—review. *J. Mater. Chem.* **2011,** *21* (40).
10. Arepalli, S., Laser Ablation Process for Single-Walled Carbon Nanotube Production. *J. Nanosci. Nanotech.* **2004,** *4* (4), 317-325.
11. Das, R.; Shahnavaz, Z.; Ali, M. E.; Islam, M. M.; Abd Hamid, S. B., Can We Optimize Arc Discharge and Laser Ablation for Well-Controlled Carbon Nanotube Synthesis? *Nanoscale Res Lett* **2016,** *11* (1), 510.
12. Jourdain, V.; Bichara, C., Current understanding of the growth of carbon nanotubes in catalytic chemical vapour deposition. *Carbon* **2013,** *58*, 2-39.
13. Meyyappan, M.; Delzeit, L.; Cassell, A.; Hash, D., Carbon nanotube growth by PECVD: a review. *Plasma Sources Sci. Technol.* **2003,** *12*, 205–216.
14. Khalilov, U.; Bogaerts, A.; Hussain, S.; Kovacevic, E.; Brault, P.; Boulmer-Leborgne, C.; Neyts, E. C., Nanoscale mechanisms of CNT growth and etching in plasma environment. *J Phys D Appl Phys* **2017,** *50* (18).
15. Khalilov, U.; Bogaerts, A.; Neyts, E. C., Atomic-scale mechanisms of plasma-assisted elimination of nascent base-grown carbon nanotubes. *Carbon* **2017,** *118*, 452-457.
16. Kato, T.; Hatakeyama, R., Growth of Single-Walled Carbon Nanotubes by Plasma CVD. *J Nanotechnol* **2010,** *2010*, 1-11.
17. Khalilov, U.; Bogaerts, A.; Xu, B.; Kato, T.; Kaneko, T.; Neyts, E. C., How the alignment of adsorbed ortho H pairs determines the onset of selective carbon nanotube etching. *Nanoscale* **2017,** *9* (4), 1653-1661.
18. Behr, M. J.; Gaulding, E. A.; Mkhoyan, K. A.; Aydil, E. S., Hydrogen etching and cutting of multiwall carbon nanotubes. *Journal of Vacuum Science & Technology B, Nanotechnology and Microelectronics: Materials, Processing, Measurement, and Phenomena* **2010,** *28* (6), 1187-1194.
19. Hou, P. X.; Li, W. S.; Zhao, S. Y.; Li, G. X.; Shi, C.; Liu, C.; Cheng, H. M., Preparation of metallic single-wall carbon nanotubes by selective etching. *ACS Nano* **2014,** *8* (7), 7156-62.
20. Zhang, G.; Mann, D.; Zhang, L.; Javey, A.; Li, Y.; Yenilmez, E.; Wang, Q.; McVittie, J. P.; Nishi, Y.; Gibbons, J.; Dai, H., Ultra-high-yield growth of vertical single-walled carbon nanotubes: Hidden roles of hydrogen and oxygen. *Proc Natl Acad Sci U S A* **2005,** *102* (45), 16141-5.
21. Kimura, R.; Hijikata, Y.; Eveleens, C. A.; Page, A. J.; Irle, S., Chiral-selective etching effects on carbon nanotube growth at edge carbon atoms. *J Comput Chem* **2019,** *40* (2), 375-380.
22. Khalilov, U.; Vets, C.; Neyts, E. C., Molecular evidence for feedstock-dependent nucleation mechanisms of CNTs. *Nanoscale Horiz.* **2019**.
23. Zhang, G.; Qi, P.; Wang, X.; Lu, Y.; Li, X.; Tu, R.; Bangsaruntip, S.; Mann, D.; Zhang, L.; Dai, H., Selective etching of metallic carbon nanotubes by gas-phase reaction. *Science* **2006,** *314* (5801), 974-7.
24. Ding, L.; Tselev, A.; Wang, J.; Yuan, D.; Chu, H.; McNicholas, T. P.; Li, Y.; Liu, J., Selective growth of well-aligned semiconducting single-walled carbon nanotubes. *Nano Lett* **2009,** *9* (2), 800-5.

25. Zhou, W.; Zhan, S.; Ding, L.; Liu, J., General rules for selective growth of enriched semiconducting single walled carbon nanotubes with water vapor as in situ etchant. *J Am Chem Soc* **2012,** *134* (34), 14019-26.
26. Che, Y.; Wang, C.; Liu, J.; Liu, B.; Lin, X.; Parker, J.; Beasley, C.; Wong, H. S.; Zhou, C., Selective synthesis and device applications of semiconducting single-walled carbon nanotubes using isopropyl alcohol as feedstock. *ACS Nano* **2012,** *6* (8), 7454-62.
27. Wang, B.; Poa, C. H.; Wei, L.; Li, L. J.; Yang, Y.; Chen, Y., (n,m) Selectivity of single-walled carbon nanotubes by different carbon precursors on Co-Mo catalysts. *J Am Chem Soc* **2007,** *129* (29), 9014-9.
28. Liu, C.; Cheng, H. M., Controlled Growth of Semiconducting and Metallic Single-Wall Carbon Nanotubes. *J Am Chem Soc* **2016,** *138* (21), 6690-8.
29. Xu, Z.; Qiu, L.; Ding, F., The kinetics of chirality assignment in catalytic single-walled carbon nanotube growth and the routes towards selective growth. *Chem Sci* **2018,** *9* (11), 3056-3061.
30. Yang, F.; Wang, X.; Si, J.; Zhao, X.; Qi, K.; Jin, C.; Zhang, Z.; Li, M.; Zhang, D.; Yang, J.; Zhang, Z.; Xu, Z.; Peng, L. M.; Bai, X.; Li, Y., Water-Assisted Preparation of High-Purity Semiconducting (14,4) Carbon Nanotubes. *ACS Nano* **2017,** *11* (1), 186-193.
31. Maruyama, S.; Kojima, R.; Miyauchi, Y.; Chiashi, S.; Kohno, M., Low-temperature synthesis of high-purity single-walled carbon nanotubes from alcohol. *Chem. Phys. Lett.* **2002,** *360*, 229–234.
32. Hou, B.; Wu, C.; Inoue, T.; Chiashi, S.; Xiang, R.; Maruyama, S., Extended alcohol catalytic chemical vapor deposition for efficient growth of single-walled carbon nanotubes thinner than (6,5). *Carbon* **2017,** *119*, 502-510.
33. Bal, K. M.; Neyts, E. C., On the time scale associated with Monte Carlo simulations. *J Chem Phys* **2014,** *141* (20), 204104.
34. Neyts, E. C.; Bogaerts, A., Combining molecular dynamics with Monte Carlo simulations: implementations and applications. *Theor. Chem. Acc.* **2012,** *132* (2).
35. Zou, C.; Shin, Y. K.; van Duin, A. C. T.; Fang, H.; Liu, Z.-K., Molecular dynamics simulations of the effects of vacancies on nickel self-diffusion, oxygen diffusion and oxidation initiation in nickel, using the ReaxFF reactive force field. *Acta Materialia* **2015,** *83*, 102-112.
36. Wagner, R. S.; Ellis, W. C., Vapor-Liquid-Solid Mechanism of Single Crystal Growth. *Applied Physics Letters* **1964,** *4* (5), 89-90.
37. Bussi, G.; Donadio, D.; Parrinello, M., Canonical sampling through velocity rescaling. *J Chem Phys* **2007,** *126* (1), 014101.
38. Khalilov, U.; Bogaerts, A.; Neyts, E. C., Microscopic mechanisms of vertical graphene and carbon nanotube cap nucleation from hydrocarbon growth precursors. *Nanoscale* **2014,** *6* (15), 9206-14.
39. Luo, M.; Penev, E. S.; Harutyunyan, A. R.; Yakobson, B. I., Effect of Cap–Catalyst Structural Correlation on the Nucleation of Carbon Nanotubes. *The Journal of Physical Chemistry C* **2017,** *121* (34), 18789-18794.
40. Buffat, P.; Borel, J. P., Size effect on the melting temperature of gold particles. *Physical Review A* **1976,** *13* (6), 2287-2298.
41. Shibuta, Y.; Suzuki, T., A molecular dynamics study of the phase transition in bcc metal nanoparticles. *J Chem Phys* **2008,** *129* (14), 144102.
42. Neyts, E. C., Plasma-Surface Interactions in Plasma Catalysis. *Plasma Chemistry and Plasma Processing* **2016,** *36* (1), 185-212.
43. Hata, K.; Futaba, D. N.; Mizuno, K.; Namai, T.; Yumura, M.; Iijima, S., Water-assisted highly efficient synthesis of impurity-free single-walled carbon nanotubes. *Science* **2004,** *306* (5700), 1362-4.
44. Kimura, H.; Goto, J.; Yasuda, S.; Sakurai, S.; Yumura, M.; Futaba, D. N.; Hata, K., The infinite possible growth ambients that support single-wall carbon nanotube forest growth. *Sci Rep* **2013,** *3*, 3334.
45. Vonk, V.; Khorshidi, N.; Stierle, A., Structure and Oxidation Behavior of Nickel Nanoparticles Supported by YSZ(111). *J Phys Chem C Nanomater Interfaces* **2017,** *121* (5), 2798-2806.

46. Rellinghaus, B.; Stappert, S.; Wassermann, E. F.; Sauer, H.; Splietho, B., The effect of oxidation on the structure of nickel nanoparticles. *Eur. Phys. J. D* **2001,** *16*, 249-252.
47. Dean, J. A., 4. PROPERTIES OF ATOMS, RADICALS, AND BONDS. In *Lange's Handbook of Chemistry*

Fifteenth Edition ed.; McGRAW-HILL, INC.: 1999.
48. Luo, Y. R., *Comprehensive Handbook of Chemical Bond Energies*. CRC Press, Boca Raton: FL, 2007
49. Harutyunyan, A. R.; Chen, G.; Paronyan, T. M.; Pigos, E. M.; Kuznetsov, O. A.; Hewaparakrama, K.; Kim, S. M.; Zakharov, D.; Stach, E. A.; Sumanasekera, G. U., Preferential growth of single-walled carbon nanotubes with metallic conductivity. *Science* **2009,** *326* (5949), 116-20.
50. Mora, E.; Pigos, J. M.; Ding, F.; Yakobson, B. I.; Harutyunyan, A. R., Low-temperature single-wall carbon nanotubes synthesis: feedstock decomposition limited growth. *J Am Chem Soc* **2008,** *130* (36), 11840-1.
51. Zhang, L.; He, M.; Hansen, T. W.; Kling, J.; Jiang, H.; Kauppinen, E. I.; Loiseau, A.; Wagner, J. B., Growth Termination and Multiple Nucleation of Single-Wall Carbon Nanotubes Evidenced by in Situ Transmission Electron Microscopy. *ACS Nano* **2017,** *11* (5), 4483-4493.
52. Ding, F.; Larsson, P.; Larsson, J. A.; Ahuja, R.; Duan, H.; Rosen, A.; Bolton, K., The importance of strong carbon-metal adhesion for catalytic nucleation of single-walled carbon nanotubes. *Nano Lett* **2008,** *8* (2), 463-8.

TOC Image